Aerosol and Air Quality Research, 16: 212–220, 2016

ISSN: 1680-8584 print / 2071-1409 online
doi: 10.4209/aaqr.2015.06.0399

Evaluation of N95 Filtering Facepiece Respirators Challenged with Engineered Nanoparticles

Yue Zhou*, Yung Sung Cheng

Lovelace Respiratory Research Institute, 2425 Ridgecrest SE, Albuquerque, NM, 87108, USA

ABSTRACT

NIOSH-certified respirators, including N95 respirators, are recommended when engineering and administrative controls do not adequately prevent exposures to airborne nanomaterials. Laboratory evaluations of filtering efficiency using standard test aerosols have been reported in the literature, but there is no information on penetration of engineered nanoparticles (1–100 nm) for N95 filtering facepiece respirators (FFR). This project evaluated the performance of two manufacturers' N95 FFR filters challenged with engineered nanoparticle aerosols containing metal oxides (such as TiO_2) and carbon (such as fullerenes and nanotubes) in contrast with a sodium chloride (NaCl) aerosol at flow rates of 30, 85, and 130 L min^{-1}. For new respirator filters in general, NaCl aerosol penetration was less than 5% and the most penetrating particle size occurred at 40 nm. Overall penetration of the engineered nanoparticle aerosols exceeded 5% and was often greater than 5% at and near the most penetrating particle size (MPPS), which occurred at a larger particle size range (90–150 nm). For respirators treated with isopropanol in which the electrostatic force was removed, penetration of NaCl and engineered nanoparticles increased substantially and the MPPS increased to 150 nm for both types of aerosols. Our results indicated that a possible reason for higher maximum penetrations and shift of MPPS observed for these engineered nanoparticles in the new respirators was related to electrostatic collection processes.

Keywords: N95 filter; Aerosol penetration; Electret filter; Engineered nanoparticles.

INTRODUCTION

Advances in nanotechnology have produced a diverse range of nanomaterials or "engineered nanoparticles," including metal oxides, fullerenes, nanotubes, nanowires, and quantum dots (NIOSH, 2009). The explosive development of nanomaterials has raised concerns about potential exposure and associated health effects (Kreyling *et al.*, 2004; Maynard *et al.*, 2004; Hoet *et al.*, 2004; Biswas and Wu, 2005; NIOSH, 2009). Several exposure assessment studies in nanomaterial production facilities have found that concentrations of nanomaterials in workplace are generally higher than that in ambient environments (Maynard *et al.*, 2004; Demou *et al.*, 2008; Han *et al.*, 2008). Concentrations of multi-walled carbon nanotubes (MWCNT) ranged from 37 to 430 μg m^{-3} (Han *et al.*, 2008); in single-walled carbon nanotubes (SWCNT) manufacturing facilities concentrations of 0.77–53 μg m^{-3} have been reported (Maynard *et al.* 2004). Average concentrations of 188 μg m^{-3} and a peak concentration of 1.34 mg m^{-3} were measured in a metal oxide nanostructure manufacturing facility (Demou *et al.*, 2008).

Respirators have been recommended when engineering and administrative controls do not adequately prevent exposures to airborne nanomaterials (NIOSH, 2009). NIOSH certifies respirator filters at a relatively high flow rate of 85 L min^{-1} using solid sodium chloride (NaCl) or liquid dioctyl phthalate (DOP) aerosol challenges with an approximate mass median aerodynamic diameter (MMAD) of 350 nm, the most penetrating particle size (MPPS) for filters relying primarily on mechanical collection mechanisms (impaction, interception and diffusion) (Rengasamy *et al.*, 2011).

Laboratory evaluation of N95 respirators provided information on penetration efficiency as a function of particle size and flow rate showing different penetration curves for N95 respirators from different manufacturers with maximum penetrations below 5% using NaCl aerosol (Qian *et al.*, 1998). Commercial respirators usually use electrostatic-charged filter material (electret) to enhance the collection efficiency. It has been shown that NIOSH-certified N95 filtering facepiece respirators (FFR) constructed from electret filter material have a MPPS of 40 to 100 nm (Martin and Moyer, 2000). When electrostatic charges are removed by dipping the filter in isopropanol, penetration increases substantially and the MPPS increases to 200–400 nm, which is the range expected for filters relying solely on mechanical collection mechanisms (interception, impaction and diffusion)

* Corresponding author.
Tel.: +505-348-9477; Fax: +505-348-8567
E-mail address: yzhou@lrri.org

(Hinds, 1998; Martin and Moyer, 2000).

Balazy *et al.* (2006) found that several samples of N95 filters exceeded 5% penetration from NaCl aerosol at the MPPS of 40–50 nm at 85 L min^{-1}. They demonstrated that an electrostatic mechanism improved the collection efficiency of electret filters and shifted the MPPS from ~300 nm to 50 nm.

Most laboratory tests of N95 FFRs have used polydisperse NaCl or DOP test particles similar to those employed in NIOSH certification tests. One study used monodisperse silver particles as the test aerosol (Renagasamy *et al.* 2008). Very few studies tested the N95 filter performance against aerosols in the occupational environments particles such as diesel exhaust and welding fume particles. Janssen and Bidwell (2006) investigated performance of two N95 FFRs exposed to diesel engine exhaust and measured concentration of elemental carbon as index of diesel exhaust particles. Penetrations of 1.12 and 2.71% were obtained after 2- and 8- hour exposure for one respirator; for another respirator, penetrations of 12.1 and 11.5 % were obtained. Cho *et al.* (2011) compared penetration of four N95 FFRs using NaCl and welding fume particles. Penetration of welding fume particles was lower than that of sodium chloride test particles, suggesting that the sodium chloride is a conservative surrogate for weld fume. Cho *et al.* (2013) found for an N95 FFR that penetration of a glass fiber aerosol with an aerodynamic diameter of 1.73 μm was less than polystyrene latex spheres of 1.05 and 1.58 μm in a N95 filter, although all aerosols showed penetration below 5%.

The evaluation of N95 respirators showed that filter materials were electrostatically charged to enhance the particle filtration efficiency (Chen *et al.*, 1993). However, the electrostatic charges on the filter material could be neutralized or eliminated because of high temperature and high humidity, chemical treatment, and radiation exposure as well as particle loading. Surface charges on respirators stored at 38°C and >90% RH were reduced after 2 days and were eliminated in 6 days (Cheng *et al.*, 2006). It was also reported that chemical treatment with either isopropanol or Static Guard (Alberto-Culver CO., Melrose Park, IL) removed most electrostatic charges based on the particle penetration measurements (Chen *et al.*, 1993; Chen and Huang 1998; Martin and Moyer, 2000). Similar observations were also reported for an electret filter treated with ethanol (Kanaoka *et al.*, 1984). Performance in electret filters also degraded with heavy aerosol loading, leading to higher penetration (Chen *et al.*, 1993; Moyer and Bergman, 2000). Finally, N95 filters irradiated with high X-ray dose showed increased penetration (Janssen, 2004).

Although there have been studies of engineered nanoparticle collection by standardized fibrous filters not used in respirators (Kim *et al.*, 2009; Seto *et al.*, 2010), no publications describe the performance of electret filters, such as those used in N95 FFRs, when challenged with engineered nanoparticles. The purpose of this study was to compare the performance of N95 respirator filters using engineered nanoparticle and sodium chloride aerosols, as well as to investigate the impact on filter performance after removing the electrostatic charge.

MATERIAL AND METHODS

Experimental Respirator Filters

Two commercial N95 filtering facepiece respirators were selected from a current list of NIOSH certified respirators previously tested for fitting characteristics (Coffey *et al.*, 2004) with best and worst performance. To evaluate the respirator without electrostatic force, a new respirator was dipped into liquid isopropanol in a container for 1 min and dried by evaporation for at least 24 hours in a hood at room temperature before tests.

Challenge Aerosol

The test aerosols consisted of a multi-walled carbon nanotube (CNT), titanium dioxide (TiO_2) and carbon based fullerene. The CNT had a purity of > 97%, tube diameter about 10–30 nm, and tube length > 2 μm (Shenzhen Nanotech Port Co., Shenzhen, China) as used previously in mouse inhalation toxicology studies (Mitchell *et al.*, 2007) and a study of CNT deposition in a human lung replica (Su and Cheng 2014). The CNT aerosols was generated by a dry powder dispersion method using a vortex shaker (Vortex Genie 2, Model G560, Scientific Industries Inc., Bohemia, NY) (Ku *et al.*, 2006).

Fullerene material with 99% purity (Sigma-Aldrich, St Louis, MO) was generated using an evaporation and condensation method as described by Gupta *et al.* (2007). The test material was placed in a quartz boat inside a tube furnace operating at 500–550°C. A regulated air stream carried the evaporated material into a glass condensation chamber to form the aerosol (Cheng *et al.*, 1988).

The anatase TiO_2 aerosol, with a purity > 99% and 10–25 nm diameter (US Research Nanomaterials Inc., Houston, TX), was generated using the vortex dry powder generation method.

A standard sodium chloride (NaCL) test aerosol was also used for comparison. A six-jet Collison nebulizer operated at 20 psig was used to aerosolize the sodium chloride aqueous solution (0.1 mg mL^{-1}).

Particle size distribution was monitored with a scanning mobility particle sizer (SMPS, GRIMM Aerosol Technologies, Douglasville, GA). The count median diameters and geometric standard deviations (GSD) were 40 nm (GSD = 1.83) for NaCl, 58 nm (GSD = 2.10) for TiO_2, 45 nm (GSD = 2.19) for CNT and 12.3 nm (GSD = 1.38) for fullerene, respectively (Fig. 1).

Test Chamber

The experimental apparatus consisted of a test chamber, nanoparticle generator, and aerosol monitor (Fig. 2). The cylindrical test chamber was similar to that described by Cheng *et al.* (2006). A mixing fan was placed at the top of the chamber to increase aerosol uniformity. A honeycomb flow straightener was placed between the fan and the chamber to reduce the turbulence. The flow in the test chamber was laminar in the lower test section.

A manikin was placed at the bottom of the chamber with a test respirator. The manikin was equipped with a probe to sample the aerosol inside the facepiece. The outside (or

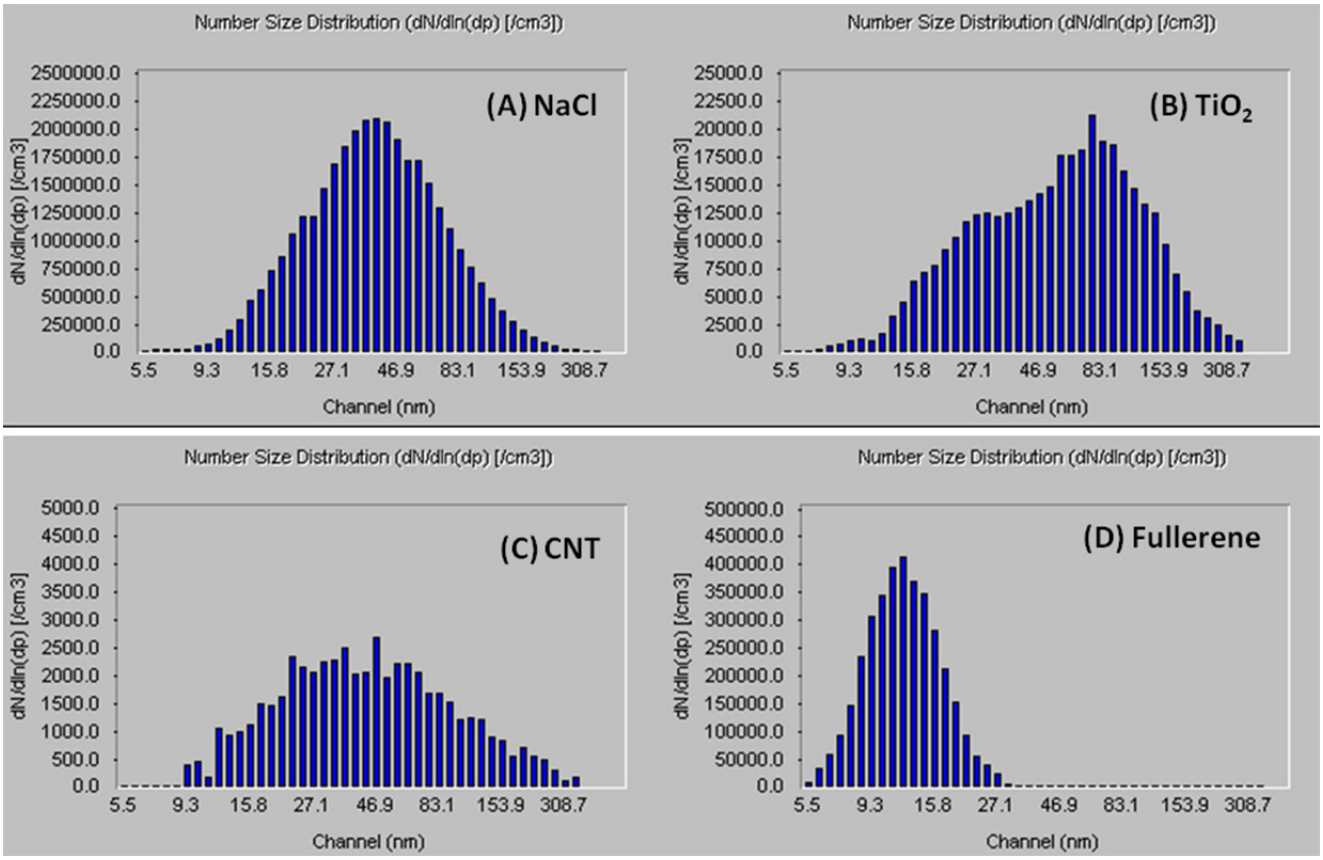

Fig. 1. Particle size distributions measured with a SMPS for NaCl (A), TiO_2 (B), CNT (C) and fullerene (D) respectively.

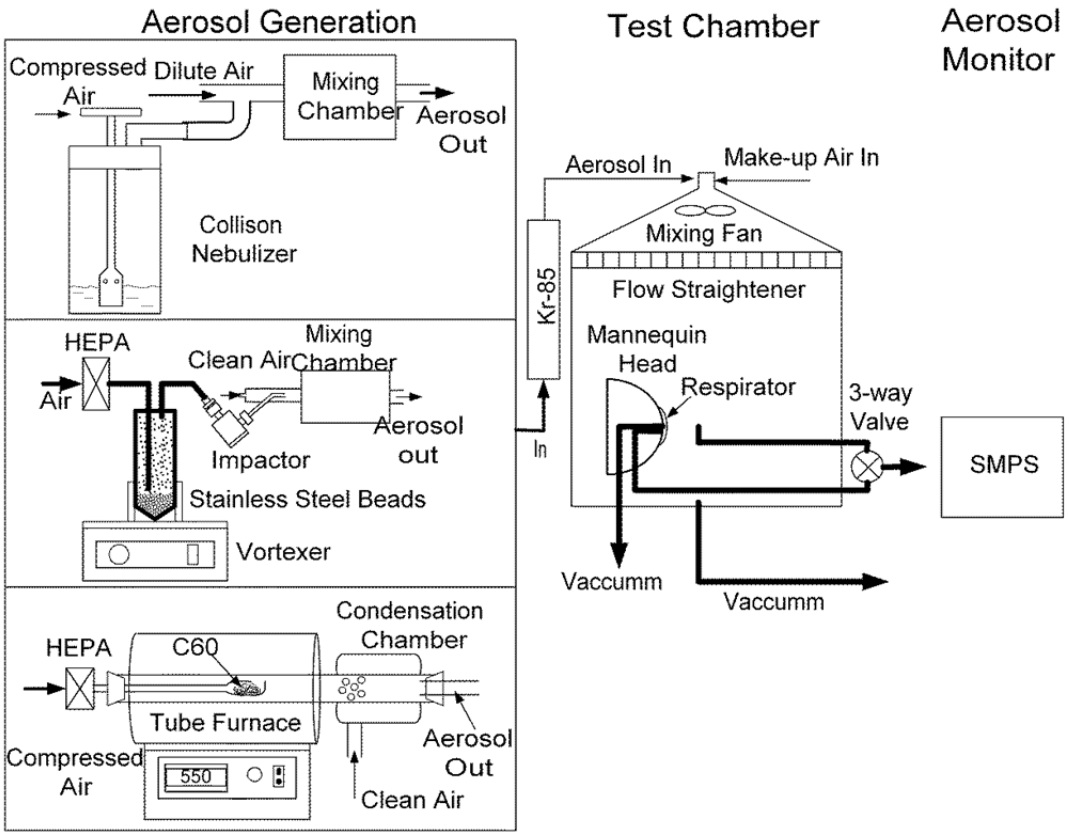

Fig. 2. Experimental setup for nanoparticle generation and penetration measurement.

chamber) aerosol concentration was sampled at 3 cm from the respirator outer surface with a probe of the same diameter and similar length as the in-facepiece sampling probe. The experiments were performed with the manikin at the inhalation flow rate provide by the vacuum. The flow rate was controlled by a flow meter.

The flow rates through the manikin were 30, 85, and 130 L min^{-1}. The 30 L min^{-1} was selected to represent low to moderate workload; 85 L min^{-1} is used for NIOSH respirator filter certification tests and represents a moderate to high workload; 130 L min^{-1} represents inhalation at a very heavy workload. It is also represents the peak inspiratory flow of a cyclic flow with a mean inspiratory flow of 85 L min^{-1} (Eshbaugh *et al.*, 2009).

Aerosol concentrations were measured with a scanning mobility particle sizer (SMPS, GRIMM Aerosol Technologies, Douglasville, GA). The test chamber and aerosol generation apparatus were placed inside a hood to prevent nanoparticles from leaking into the room. Appropriate personal protection, including respirator, eye protection, and gloves, were used when handling the nanomaterials.

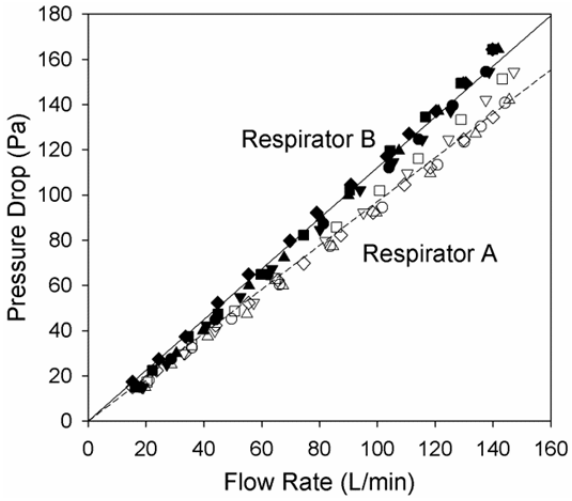

Fig. 3. Pressure drop as a function of flow rate for Respirator A (empty symbols) and Respirator B (solid symbols). Different shapes of the symbols represent each individual respirator.

Experimental Protocol

In the first series of experiments, new respirators from the package were placed on the manikins. Care was taken to seal the respirator on the manikin face with silicon sealant. The pressure drop across the facepiece as a function of flow rate was measured with a velocity meter (VelociCalc Plus 8360-M, TSI, Shoreview, MN). Penetration was determined by the ratio of aerosol concentrations inside and outside of the respirator. For each type of respirator, five different units were tested to get a range of variability from the same respirator.

Data Analysis

From replicate data of five facepieces for each experimental condition, the mean and standard deviation of each penetration measurement were calculated. The maximum penetration (P_{max}) and the MPPS for each flow rate were then determined. A statistical analysis was performed to test the null hypothesis of equal values of P_{max} for each engineered nanoparticle and the standard NaCl test aerosol at the same flow rate for each respirator model. The Student T-test was used to determine whether values of P_{max} for each engineered nanoparticle and the NaCl particle were significantly different. A p-value of < 0.05 was considered statistically significant. Similarly, the same statistical analysis of values of the P_{max} between Respirator A and Respirator B for each experimental condition was made to determine whether there was a significant difference between these two respirators.

RESULTS

Pressure Drop

Fig. 3 plots measured pressure drop as a function of inspiratory flow rate for both test respirators showing the data scattering of pressure drops for each of the five units per respirator type. This may be due to variations in filter structure of the individual filters. Also, the pressure drop of Respirator B was higher than those of Respirator A. The pressure drop was a linear function of the flow rate for both respirators.

New N95 Respirators

The standard deviations for five units of the same respirator were relatively large, indicating that these filters may vary in their structures (Figs. 4(A)–4(D)). For all of the respirator filters, NaCl aerosol penetration increased with increasing flow rate. Maximum penetration at all test flows occurred at around 43 nm. Respirator A showed the highest penetration (4%) at 130 L min^{-1} and penetration for this respirator was significantly higher than for Respirator B at 85 and 130 L min^{-1}. There was no significant difference between maximum penetration (P_{max}) values for Respirators A and B at 30 L min^{-1} (Fig. 4(A)).

The two respirators showed similar penetration of the TiO_2 aerosol. Maximum penetration occurred at around 154 nm and exceeded 5% at 85 and 130 L min^{-1}. Penetration of 91 nm TiO_2 particles was also greater than 5% at 130 L min^{-1} for both respirators. The maximum penetration at each particle size and flow rate was similar for the two respirators (Fig. 4(B)).

In Fig. 4(C) two respirator filters exhibited similar penetration of CNT aerosol. Maximum penetration at the MPPS of 91 nm exceeded 5% at flow rates of 130 L min^{-1} and 85 L min^{-1}. At 130 L min^{-1} flow, all five Respirator A units and four of five Respirator B units exceeded 5% penetration. At 85 L min^{-1} flow, two of the five Respirator A units and two of the five Respirator B units exceeded 5% penetration. Mean penetrations for 154 nm CNT particles in both respirators also exceeded 5% at the highest flow rate of 130 L min^{-1}. The maximum penetration at 91 nm was 8.7 ± 2.8% for Respirator A and 7.8 ± 3.1% for Respirator B. There were no significant difference of P_{max} values between Respirator A and B in all three flow rates.

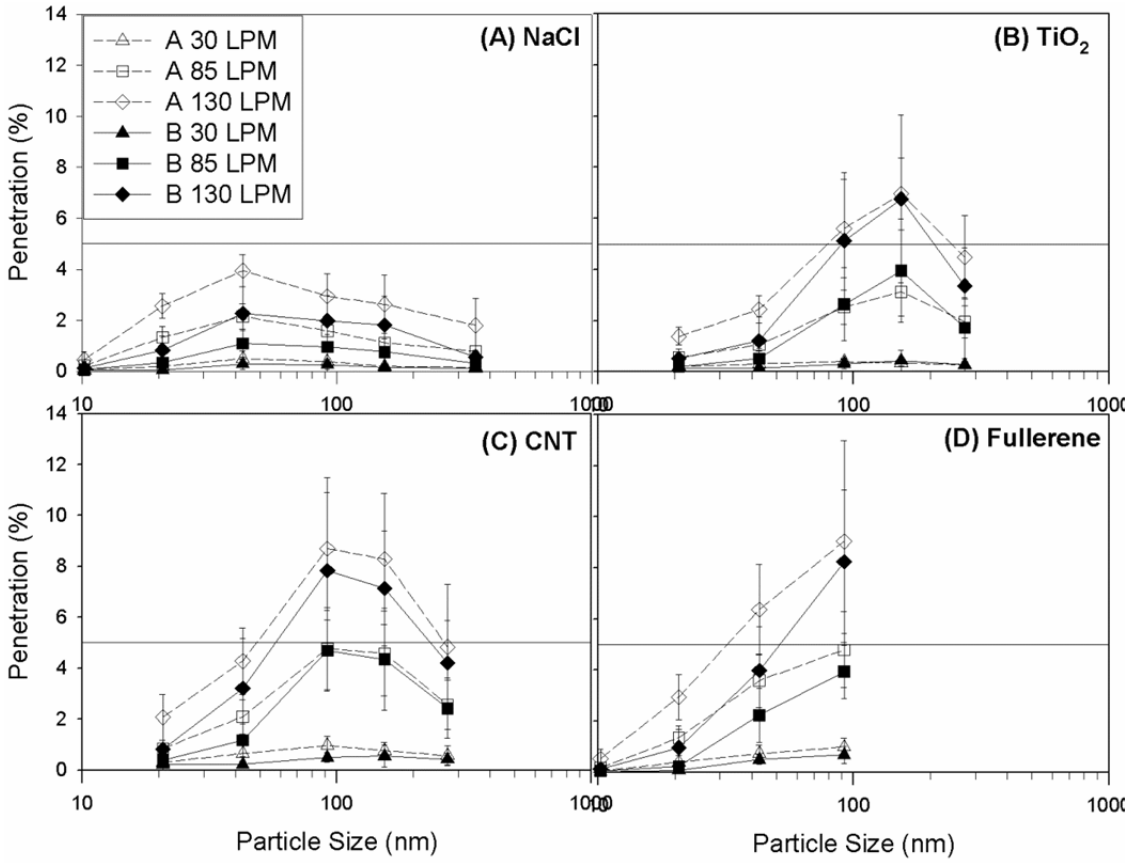

Fig. 4. Penetration of NaCl (A), TiO_2 (B), CNT (C) and fullerene (D) in both Respirator A and B as a function of particle diameter and flow rate. Each data point shows the mean and standard deviation of 5 new units from Respirator A (empty symbols) and Respirator B (solid symbols).

Fig. 4(D) shows the penetration against fullerene nanoparticles. There was no penetration data for particles > 100 nm as the concentration of fullerene dropped to a very low level. Penetrations through Respirator A were generally higher than Respirator B, but within the experimental errors. Penetration exceeded 5% for 91 nm at flow rate of 130 L min^{-1} and 85 L min^{-1}. At 130 L min^{-1} flow, four of the five Respirator A units and four of the five Respirator B units exceeded 5% penetration for 91 nm particles. At 85 L min^{-1} flow, two of the five Respirator A units and none of the five Respirator B units exceeded 5% penetration for 91 nm particles. The MPPS could not be determined from the measurement but was ≥ 91 nm. There was no significant difference in P_{max} values at 91 nm between Respirator A and B in all three flow rates.

The maximum penetration of engineered nanoparticles was higher than those measured for NaCl in both Respirator A and B. Also penetration of these engineered nanoparticles often exceeded 5% at and near the MPPS at flow rates of 130 and 85 L min^{-1}. The maximum penetration of NaCl did not exceed 5%. There was also a shift of MPPS from about 40 nm for NaCl aerosol to about 90–150 nm for engineered nanoparticles. The values of P_{max} at MPPS for TiO_2 and CNT nanoparticles were significantly higher than those for the NaCl particle at all three flow rates in both Respirator A and B ($p < 0.05$). The MPPS value for the fullerene particle could not be determined from the current measurement, but the P_{max} values at 91 nm for fullerene were significantly higher than P_{max} values at the MPPS of 43 nm for the NaCl particle in all three flow rates in both Respirator A and B ($p < 0.05$).

Treated N95 Respirators

Fig. 5(A) shows NaCl aerosol penetration through Respirator A after treatment with isopropanol, indicating substantial increase of penetration and shift of MPPS to larger particle size as compared to the results without treatment (Fig. 4(A)). A maximum of 49% penetration was measured at MPPS of 154 nm for a flow rate of 130 L min^{-1}. At the 85 L min^{-1} test flow rate, the maximum penetration at the MPPS of 273 nm was increased from about 2% to 40% after the respirator was treated. This was similar to what was reported by Martin and Moyer (2000) for a N95 filter (Manufacturer A).

Figs. 5(B) and 5(C) show similar penetration data for TiO_2 and CNT nanoparticles at three different flow rates. The MPPS of both nanoparticles were 154 nm. Maximum penetration at 130 L min^{-1} was 51 and 56% for TiO_2 and CNT, respectively, substantially higher than 7 and 8% before treatment. The penetration of the fullerene aerosol (Fig. 5(D)) was substantially higher than before isopropanol treatment.

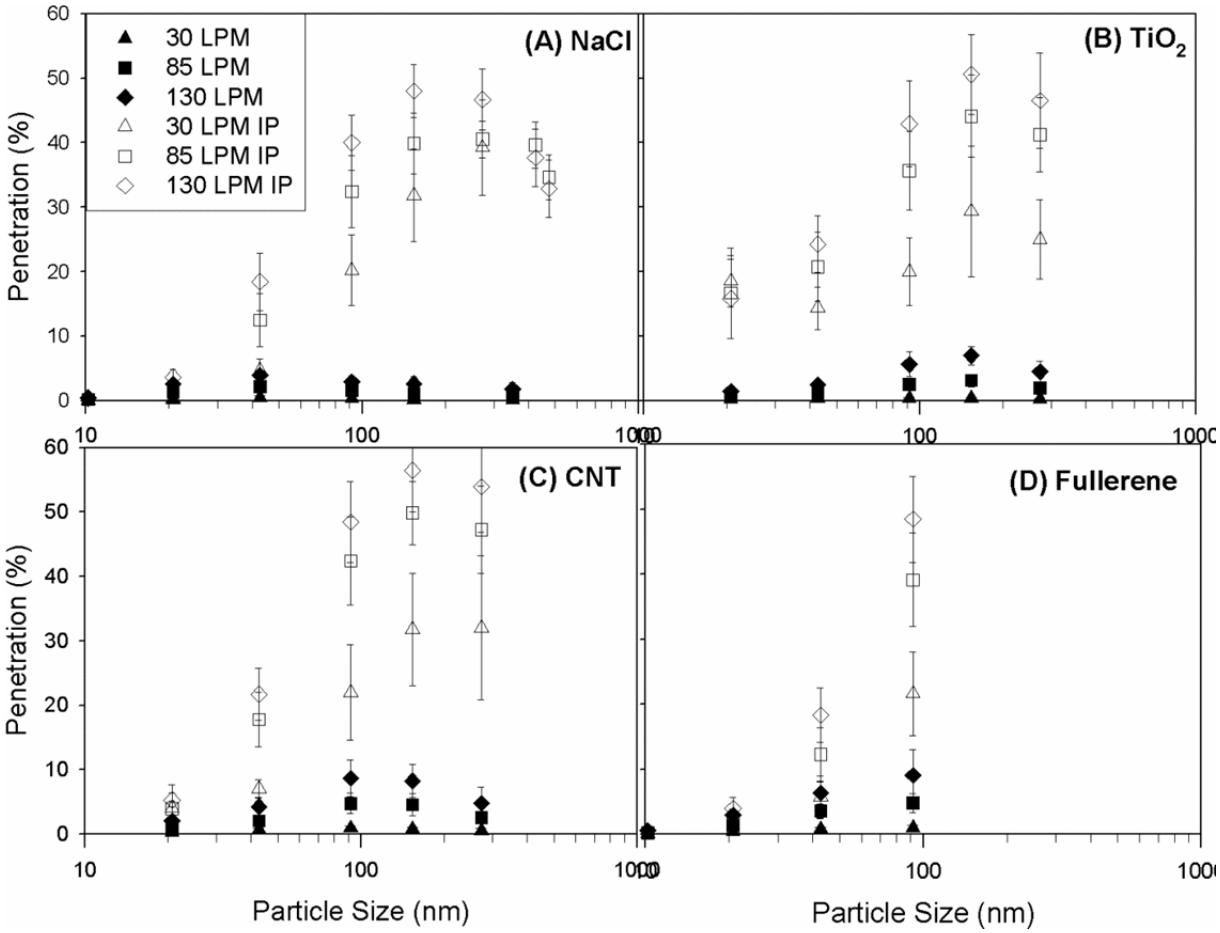

Fig. 5. Penetration of NaCl (A), TiO_2 (B), CNT (C) and fullerene (D) in Respirator A treated with isopropanol to remove electrostatic charges as a function of particle diameter and flow rate (empty symbols). Each data point shows the mean and standard deviation of 5 units. The penetration of new respirator (solid symbols) is also shown as a comparison.

Penetration results for Respirator B were similar to those of Respirator A (Figs. 6(A)–6(D)) Maximum penetration increased from 2.3 to 33% for NaCl aerosol, 6.8 to 28% for TiO_2, and 7.8 to 37% for CNT. The MPPS of NaCl, TiO_2 and CNT was 154 nm. Statistical comparison of values of P_{max} at the MPPS (154 nm) between TiO_2 and NaCl particles in all three flow rates showed no significant differences. Similarly, values of P_{max} at the MPPS (154 nm) between CNT and NaCl particles in all three flow rates showed no significant difference.

Before the isopropanol treatment, penetration was similar for both respirators at all flow rates and for all aerosols (Figs. 4(A) –4(D)). After treatment, penetration of all aerosols at all flow rates was greater for Respirator A in comparison to Respirator B. Values of P_{max} of Respirator A and B in the same experimental condition were significantly different ($p < 0.05$).

DISCUSSION

For both respirators in their original condition, the MPPS using NaCl test aerosol was around 40 nm, which is similar to the 40 to100 nm range reported by other investigators for similar respirator filters and experimental conditions (Martin and Moyer, 2000; Balazy *et al.*, 2006; Huang *et al.*, 2007, Eshbaugh *et al.*, 2009; Renagasamy *et al.*, 2009). After treatment with isopropanol, the MPPS for both respirators increased to 154 nm. A similar shift of the MPPS to a larger particle size for N95 respirator filters challenged with a NaCl aerosol was reported by Martin and Moyer (2000).

The main discovery in this study was that maximum penetrations of TiO_2, CNT and fullerene were higher than those measured for NaCl in untreated Respirator A and B. Also, penetration of these nanoparticles often exceeded 5% at and near the MPPS in 130 and 85 L min^{-1} flow rates. The maximum penetration of NaCl did not exceed 5% in any of the three flow rates. There was also a shift of MPPS from 43 nm for NaCl aerosol to about 91-154 nm for engineered nanoparticles. This was quite different from a reported study where real world aerosol encountered in occupational environments was tested. Penetrations for NIOSH-approved N95 filtering facepiece respirators were lower for welding fume particles (Cho *et al.*, 2011) than for NaCl test aerosol.

On the other hand, for charge-neutralized N95 Respirator A and B, values of P_{max} at the MPPS (154 nm) between TiO_2 and NaCl particles at any of the three flow rates

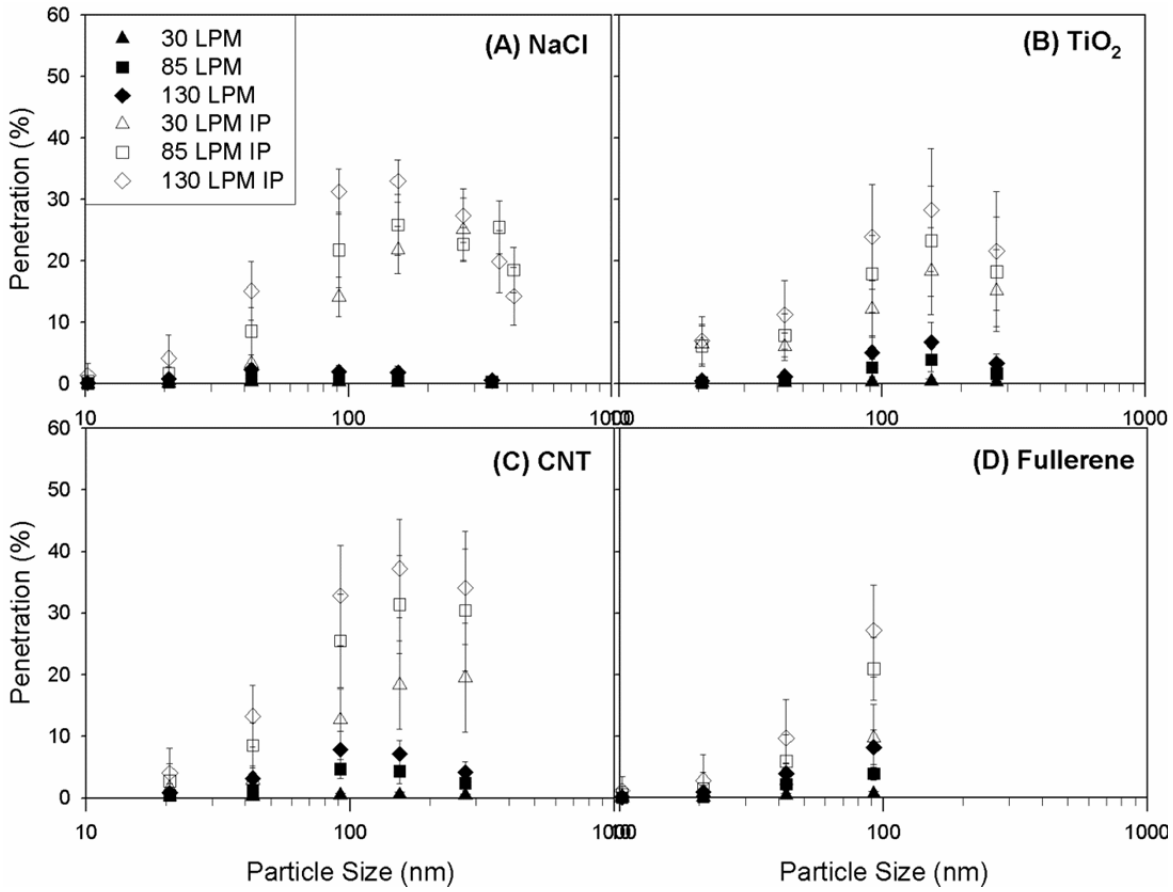

Fig. 6. Penetration of NaCl (A), TiO_2 (B), CNT (C) and fullerene (D) in Respirator B treated with isopropanol to remove electrostatic charges as a function of particle diameter and flow rate (empty symbols). Each data point shows the mean and standard deviation of 5 units. The penetration of new respirator (solid symbols) is also shown as a comparison.

showed no significant differences ($p > 0.05$). Similarly, values of P_{max} at the MPPS (154 nm) between CNT and NaCl particles at any of the three flow rates showed no significant differences. For fullerene nanoparticles, the peak penetration values could not be obtained from this study, but penetration appeared to be similar to those of NaCl particles for the same flow rate and particle size.

Based on these results, it seems that a possible reason for higher maximum penetrations and shift of MPPS observed for these engineered nanoparticles in the new respirators was related to electrostatic collection processes and not the mechanical processes. Particle shape and effective density may affect the penetration. However, the effection could be limited because no significant differences were found when electrostatic force was removed. If there was higher electrostatic collection processes for NaCl particles than those of engineered particles due to their electrical properties, this would explain higher penetration observed for engineered particles. There were no reported studies on the shift of MPPS in electret filters for aerosols of different materials. The shift of MPPS for these nanoparticles could also be related to the electrostatic collection processes although the exact mechanism was not clear. Further investigation into effects of aerosol materials on the electrostatic collection processes are needed to fully understand and explain the observed differences in P_{max} and MPPS between NaCl aerosol and engineered nanoparticles.

Values of P_{max} between untreated Respirator A and B for the same experimental condition (type of particle and flow rate) were not significantly different except in the case of NaCl particles at 130 and 85 L min^{-1} (Fig. 4(A)). After the treatment, penetrations for Respirator A were higher than Respirator B. Values of P_{max} of Respirator A and B for the same experimental condition were significantly different ($p < 0.05$). When these respirators were treated with isopropanol to remove electrostatic charges, the main particle filtration mechanisms were mechanical processes that included diffusion, interception and inertial mechanism (Chen and Huang 1998; Balazy *et al.*, 2006). Mechanical processes depend on filter characteristics, including fiber diameter, solid volume fraction and filter thickness. Fig. 3 also showed that Respirator A had lower pressure drop. Electrostatic charges are added to these filters to enhance the collection performance so that both respirators reach the 95% collection efficiency requirement for NaCl test aerosol at 85 L min^{-1}. Our results showed that at 85 L min^{-1} electrostatic collection accounted for an additional 38% and 25% of collection at MPPS for Respirator A and Respirator B, respectively.

A major implication of our observations on higher maximum penetration often exceeding 5% for these

engineered nanoparticles at 85 and 130 L min^{-1} is the effectiveness of respiratory protection using these N95 respirators with electret filter materials. These engineered particles have MPPS in the range of 90 to 150 nm. Particles in this size range can penetrate the upper respiratory tract and deposit in the pulmonary region of the human respiratory tract according to the ICRP Lung Model (ICRP, 1994) with potential health concerns. Additional studies on N95 respirator performance against engineered nanoparticles are needed to confirm the findings reported here.

CONCLUSIONS

In summary, maximum penetrations of TiO_2, CNT and fullerene were higher than those measured for NaCl aerosol for two NIOSH-approved filtering facepiece respirators. Also, penetration of these nanoparticles often exceeded 5% at and near the MPPS at flow rates of 85 and 130 L min^{-1}. The maximum penetration of NaCl aerosol did not exceed 5% at any test flow rates. There was also a shift of MPPS from about 40 nm for NaCl aerosol to about 90–150 nm for engineered nanoparticles. After respirators were treated with isopropanol to remove electrostatic charges, penetrations of NaCl and engineered nanoparticles increased substantially. The MPPS also shifted to around 150 nm. Our results indicated that a possible reason for higher maximum penetrations and shift of MPPS observed for these engineered nanoparticles in the new respirators was related to electrostatic collection processes. Further investigation into effects of aerosol materials on the electrostatic collection processes will be pursued to understand and explain the observed differences in P_{max} and MPPS. Higher penetration for these engineered nanoparticles raised some concerns of effectiveness of some N95 respirators.

ACKNOWLEDGEMENTS

This research was sponsored by U.S. NIOSH grant R01 OH009801 and OH010062.

REFERENCES

Balazy, A., Toivola, M., Reponen, T., Podgorski, A., Zimmer, A. and Grinshpun, S.A. (2006). Manikin-based Performance Evaluation of N95 Filtering-facepiece Respirators Challenged with Nanoparticles. *Ann. Occup. Hyg.* 50: 259–269.

Chen, C.C., Lehtimaki, M. and Willeke, K. (1993). Loading and Filtration Characteristics of Filtering Facepieces. *Am. Ind. Hyg. Assoc. J.* 54: 51–60.

Chen, C.C. and Huang, S.H. (1998). The Effects of Particle Charge on the Performance of a Filtering Facepiece. *Am. Ind. Hyg. Assoc. J.* 59: 227–233.

Cheng, Y.S., Yamada, Y., Yeh, H.C. and Swift, D.L. (1988). Diffusional Deposition of Ultrafine Aerosols in a Human Nasal Cast. *J. Aerosol Sci.* 19: 741–751.

Cheng, Y.S., Holmes, T.D. and Fan, B.J. (2006). Evaluation of Respirator Filters for Asbestos Fibers. *J. Occup. Environ. Hyg*. 3: 26–35.

Cho, H.W., Yoon, C.S., Lee, J.H., Lee, S.J., Viner, A. and Johnson, E.W. (2011). Comparison of Pressure Drop and Filtration Efficiency of Particulate Respirators Using Welding Fumes and Sodium Chloride. *Ann. Occup. Hyg.* 55: 666–680.

Cho, K.J., Turkevich, L., Miller, M., McKay, R., Grinshpun. S.A., Ha, K. and Reponen, T. (2013). Penetration of Fiber versus Spherical Particles through Filter Media and Faceseal Leakage of N95 Filtering Facepiece Respirators with Cyclic Flow. *J. Occup. Environ. Hyg*. 10: 109–115.

Demou, E., Peter, P. and Hellweg, S. (2008). Exposure to Manufactured Nanostructured Particles in an Industrial Pilot Plant. *Ann. Occup. Hyg.* 52: 695–606.

Eshbaugh, J.P., Gardner, P.D., Richardson, A.W. and Hofacre, K.C. (2009). N95 and P100 Respirator Filter Efficiency under Constant and Cyclic Flow. *J. Occup. Environ. Hyg*. 6: 52–61.

Gupta, A., Forsythe, W.C., Clark, M.L., Dill, J.A. and Baker, G.L. (2007). Generation of C60 Nanoparticle Aerosol in High Mass Concentrations. *J. Aerosol Sci.* 38: 592–603.

Han, J.H., Lee, E.J., Lee, J.H., So, K.P., Lee, Y.H., Bae, G.N., Lee, S.B., Ji, J.H., Cho, M.H. and Yu, I.J. (2008). Monitoring Multiwalled Carbon Nanotube Exposure in Carbon Nanotube Research Facility. *Inhalation Toxicol*. 20: 741–749.

Hinds WC (1998). *Aerosol Technology* 2nd Ed, John Wiley & Sons Inc., New York.

Hoet, P.H.M., Ruske-Hohlfeld, I. and Salata, O.V. (2004). Nanoparticles - Known and Unknown Health Risks. *J Nanobiotechnology* 2: 12.

Huang, S.H., Chen, C.W., Chang, C.P., Lai, C.Y. and Chen, C.C. (2007). Penetration of 4.5 nm to 10 μm Aerosol Particles through Fibrous Filters. *J. Aerosol Sci.* 38: 719–727.

ICRP (1994). Human Respiratory Tract Model for Radiological Protection, Publication 66, Annals of ICRP.

Janssen, J. (2004). Efficiency and Pressure Drop Effects of High Concentrations of Cement Dust on N95 Electret Filters. *J. Int. Soc. Resp. Protect.* 21: 75–82.

Janssen, J. and Bidwell, J. (2006). Performance of Four Class 95 Electret Filters Against Diesel Particulate Matter. *J. Int. Soc. Resp. Protect.* 23: 21–29.

Kanaoka, C., Emi, H. and Ishiguro, T. (1984). Time Dependency of Collection Performance of Electret Filter. In *Aerosol*, Liu, B.Y.H., Pui ,D.Y.H. and Fissan, H.J. (Eds.), Elseiver Science Publishing, New York, pp. 613–616.

Kim, S.C., Wang, J., Emery, M.S., Shin, W.G., Mulholland, G.W. and Pui, D.Y.H. (2009). Structural Property Effect of Nanoparticle Agglomerates on Particle Penetration through Fibrous Filter. *Aerosol Sci. Technol.* 43: 344–355.

Kreyling, W., Semmler, M. and Moller, W. (2004). Dosimetry and Toxicology of Ultrafine Particles. *J. Aerosol Med*. 17: 140–152.

Ku, B.K., Emery, M.S., Maynard, A.D., Stolzenburg, M.R. and McMurry, P.H. (2006). In Situ Structure Characterization of Airborne Carbon Nanofibres by a Tandem Mobility-mass Analysis. *Nanotechnol* 17: 3613–

3621.

Martin, S.B. and Moyer, E.S. (2000). Electrostatic Respirator Filter Media: Filter Efficiency and Most Penetrating Particle Size Effects. *Appl. Occup. Environ. Hyg*. 15: 609–617.

Maynard, A.D., Baron, P.A., Foley, M., Shvedova, A.A., Kisin, E.R. and Casuccio, G.S. (2004). Exposure to Carbon Nanotube Material: Aerosol Release during the Handling of Unrefined Single-walled Carbon Nanotube Material. *J. Toxicol. Environ. Health* 67A: 87–107.

Mitchell, L.A., Gao, J., Wal, R.V., Gigliotti, A., Burchiel, S.W. and McDonald, J.D. (2007). Pulmonary and Systemic Immune Response to Inhaled Multiwalled Carbon Nanotubes. *Toxicol. Sci*. 100: 203–214.

Moyer, E.S. and Bergman, M.S. (2000). Electrostatic Filter Media Efficiency Degradation Resulting from Intermittent Sodium Chloride Aerosol Exposure. *Appl. Occup. Environ. Hyg*. 15: 600–608.

NIOSH (2009). Approaches to Safe Nanotechnology. In 4 edn. National Institute for Occupational Safety and Health, CDC, Cincinnati, OH.

Qian, Y., Willeke, K., Grinshpun, S.A., Donnelly, J. and Coffey, C.C. (1998). Performance of N95 Respirators; Filtration Efficiency of Airborne Microbial and Inert Particles. *Am. Ind. Hyg. Assoc. J.* 59: 128–132.

Renagasamy, A., Eimer, B. and Shaffer, R.E. (2009). Comparison of Nanoparticle Performance of NIOSH-Approved and CE Marked Filtering-facepiece Respirators against 4-30 Nanometer Size Nanoparticles. *Ann. Occup. Hyg.* 53: 117–128.

Renagasamy, A., King, W.P., Eimer, B. and Shaffer, R.E. (2008). Filtration Performance of NIOSH-approved N95 Filtering-facepiece Respirators against 4-30 Nanometer Size Nanoparticles. *J. Occup. Environ. Hyg*. 5: 556–564.

Renagasamy, A., Miller, A. and Eimer, B. (2011). Evaluation of the Filtration Performance of NIOSH Approved N95 Filtering Facepiece Respirators by Photometric and Number-based Test Methods. *J. Occup. Environ. Hyg*. 8: 23–30.

Seto, T., Furukawa, T., Otani, Y., Uchida, K. and Endo, S. (2010). Filtration of Multi-walled Carbon Nanotube Aerosol by Fibrous Filters. *Aerosol Sci. Technol*. 44: 734–740.

Su, W.C. and Cheng, Y.S. (2014). Estimation of Carbon Nanotubes Deposition in a Human Respiratory Tract Replica. *J. Aerosol Sci.* 79: 72–85.

Received for review,June 9, 2015
Revised, July 29, 2015
Accepted, July 30, 2015